Journal of Biomedical Optics

SPIEDigitalLibrary.org/jbo

Extratympanic observation of middle ear structure using a refractive index matching material (glycerol) and an infrared camera

Soo-Keun Kong
Kyong-Myong Chon
Eui-Kyung Goh
Il-Woo Lee
Soo-Geun Wang

SPIE

Extratympanic observation of middle ear structure using a refractive index matching material (glycerol) and an infrared camera

Soo-Keun Kong, Kyong-Myong Chon, Eui-Kyung Goh, Il-Woo Lee, and Soo-Geun Wang*
Pusan National University, School of Medicine and Medical Research Institute, Department of Otorhinolaryngology Head and Neck Surgery, 179 Gudeok-ro, Seo-Gu, Busan 602739, Republic of Korea

Abstract. High-resolution computed tomography has been used mainly in the diagnosis of middle ear disease, such as high-jugular bulb, congenital cholesteatoma, and ossicular disruption. However, certain diagnoses are confirmed through exploratory tympanotomy. There are few noninvasive methods available to observe the middle ear. The purpose of this study was to investigate the effect of glycerol as a refractive index matching material and an infrared (IR) camera system for extratympanic observation. 30% glycerol was used as a refractive index matching material in five fresh cadavers. Each material was divided into four subgroups; GN (glycerol no) group, GO (glycerol out) group, GI (glycerol in) group, and GB (glycerol both) group. A printed letter and middle ear structures on the inside tympanic membrane were observed using a visible and IR ray camera system. In the GB group, there were marked a transilluminated letter or an ossicle on the inside tympanic membrane. In particular, a footplate of stapes was even transilluminated using the IR camera system in the GB group. This method can be useful in the diagnosis of diseases of the middle ear if it is clinically applied through further studies. [DOI: 10.1117/1.JBO.19.5.055003]

Keywords: glycerol; refractive index matching; infrared ray.

Paper 140014RR received Jan. 8, 2014; revised manuscript received Mar. 23, 2014; accepted for publication Mar. 31, 2014; published online May 7, 2014.

1 Introduction

High resolution-computed tomography (HRCT) is the primary method used to diagnose middle ear diseases, especially high-jugular bulb, congenital cholesteatoma, and ossicular disruption. After HRCT, if middle ear disease is still suspected, exploratory tympanotomy is used to verify the diagnosis. This is also an invasive procedure used to observe the middle ear cavity directly by making a microperforation in the tympanic membrane and then inserting a camera. However, no other method is currently available to observe the middle ear cavity directly without applying either of these two invasive methods.

Since these methods cause damage to the tympanic membrane, we deduced possible alternative methods, based on the hypothesis that a noninvasive procedure, which could enable the observation of the middle ear cavity through the tympanic membrane, would be a great help in the diagnosis of diseases of the middle ear. Optical coherence tomography (OCT) is one such possible noninvasive method. OCT is used to observe a retina in an ophthalmologic field. It was reported that OCT was used by an otolaryngologist to observe the larynx[1] and the oval window.[2] OCT is a bio-diagnostic method in which cross-sectional bio-images can be obtained using a near-infrared (IR) ray, without making an incision in the tissue. Although a number of studies are being conducted regarding OCT, additional studies are still necessary for clinical applications. Since OCT allows real-time image diagnosis of the microstructure in the unit of cells, with a resolution similar to that of microscopic observation, ophthalmologists have come to view OCT as an economical bio-diagnostic method that provides high resolution when compared with computed tomography and magnetic resonance imaging.

An IR camera system is the second noninvasive method employed to diagnose diseases of the middle ear. In the light spectrum, an IR ray has a wavelength longer than 700 nm. Although invisible to human eyes, an IR ray can penetrate tissues since its wavelength is longer than that of visible light. As a result, it might be possible to use IR rays to view tissues noninvasively because it enables less light and fewer particles to be scattered.

Additionally, it is important to consider the use of refractive index matching material (RIM), which is applied to reduce optical surface reflection. It is not possible to see through the tympanic membrane using a general light source because only a part of the light penetrates the tympanic membrane, as most of the light is reflected and scattered on the tympanic membrane, causing the images to become distorted or invisible. It can be assumed that this reflection and scattering may be reduced by using an RIM, such as liquid, cement, or gel to match the optical indices between the optical fibers when connecting optical fibers.[3,4] By using one of these types of RIM, it might be possible to see all the way through the tympanic membrane.

This study employed RIM and an IR camera system, which can be applied in a relatively simple manner, to observe the structure of the middle ear without causing damage to the tympanic membrane.

*Address all correspondence to: Soo-Geun Wang, E-mail: wangsg@pusan.ac.kr

0091-3286/2014/$25.00

2 Materials and Methods

2.1 *Materials*

Five, fresh human cadavers (10 ears) were used in this study. The samples were divided into four groups: (1) the group in which the RIM, 30% glycerol (refractive index 1.456), was not used (glycerol no, GN), (2) the group in which 30% glycerol (1 ml) was applied only to the outside of the tympanic membrane (glycerol out, GO), (3) the group in which 30% glycerol (1 ml) was applied only to the inside of tympanic membrane (glycerol in, GI), and (4) the group in which 30% glycerol (1 ml) was applied to both the inside and the outside of the tympanic membrane respectively (glycerol both, GB).

2.2 *Methods*

2.2.1 *Visible and IR ray camera system*

Photos were taken with a black and white charge-coupled device (CCD) camera (Sony Black & White Super HAD CCD, Tokyo, Japan), as shown in Fig. 1. Figure 2 showed the schematic diagram of the visible and the IR ray source. The visible ray source was obtained by using a UMT-511 model (U-medical Company, Busan, Korea). This product had a dual lens system and a significantly higher light intensity than that of other models due to its improved condensing and straightening capabilities. As our IR light source, we exchanged the general light source LED that came with the UMT-511 model for an IR LED, with an 830-nm wavelength (3 W High Power IR LED, SKHITECH Corp., Bucheon, Korea).

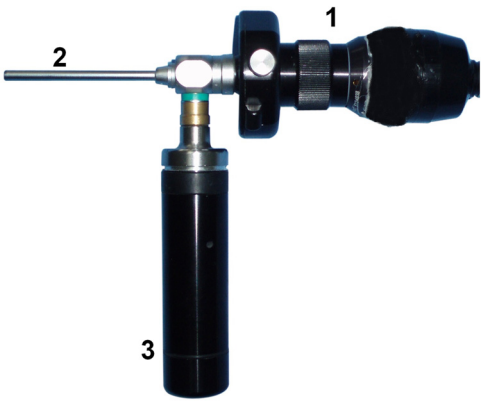

Fig. 1 System of charge-coupled device (CCD) camera. 1 Black and white CCD camera 2 Ototelescope 3 Visible or infrared (IR) ray torch.

2.2.2 *Tympanic membrane of fresh human cadavers*

After performing a retroaural incision on the fresh human cadavers, the external auditory canal (EAC) was exposed and the EAC skin was incised at the middle point of the bony EAC so that the fibrous annulus, as well as tympanomeatal flap, could be lifted up. After exposing the middle ear, a slip of paper, inscribed with a printed letter, was inserted into the middle ear. Next, the tympanomeatal flap was repositioned and the letter and the structure of the middle ear were observed.

2.2.3 *Observation using a video-ototelescopic system*

A printed letter, 3 mm in diameter, was inserted into the middle ear. Afterward, the structure of the middle ear was observed, using a 4-mm ototelescope and each of the following: a general light source [visible ray (VR)], an IR ray light source (IR ray) with black and white CCD camera.

2.2.4 *Analysis of image contrast*

To quantify achromatic contrast in each groups, we measured the grayscales of the letter and surroundings. The grayscales (G, 8-bits, range: 0 to 255) were measured using Image J (version 1.47, National Institutes of Health, Bethesda, Maryland). We measured the maximum and minimum grayscales of 10 images in each group and calculated the contrast as follows:[5]

$$\text{Contrast} = \frac{G_{max} - G_{min}}{G_{max} + G_{min}}.$$

2.2.5 *Statistical analysis*

Parametric data were analyzed using analysis of variance with Student–Newman–Keuls posthoc test. All analyses were performed using MedCalc® Software (version 10.0, Mariakerke, Belgium) and p values less than 0.01 were considered statistically significant.

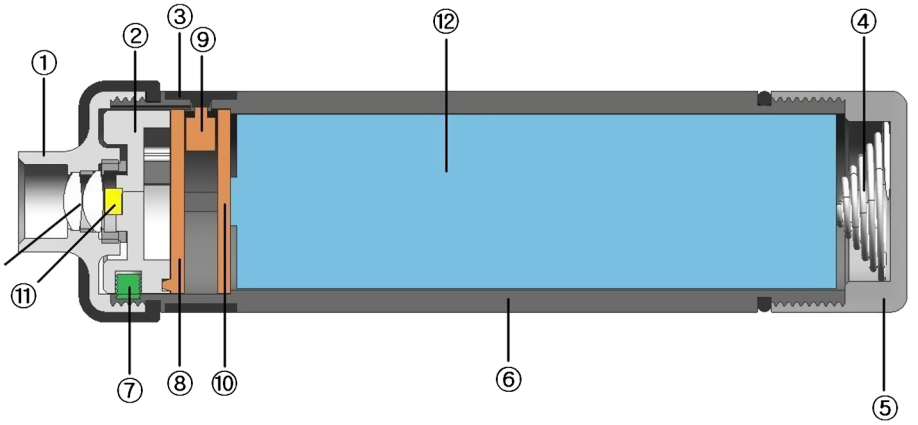

Fig. 2 Schematic view of visible and IR ray torch. 1 Joint 2 Heat sink 3 Switch button 4 Spring 5 Body cap 6 Body 7 Joint bolt 8 PCB 9 Switch 10 Connector 11 Visible or IR LED 12 Battery 13 Double lens.

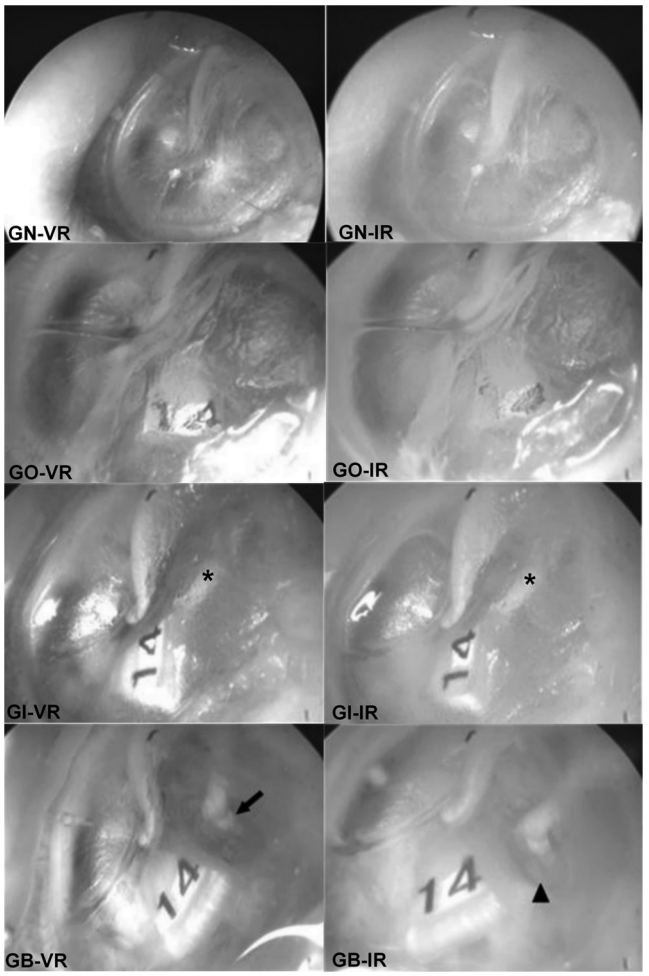

Fig. 3 The images in the left tympanic membrane of each group. Asterisk indicates the long process of incus. Arrow indicates the incudo-stapedial joint, and black arrow head indicates the footplate of stapes in the GB group. GN; glycerol no, GO; glycerol out, GI; glycerol in, GB; glycerol both, VR; visible ray, IR; IR ray.

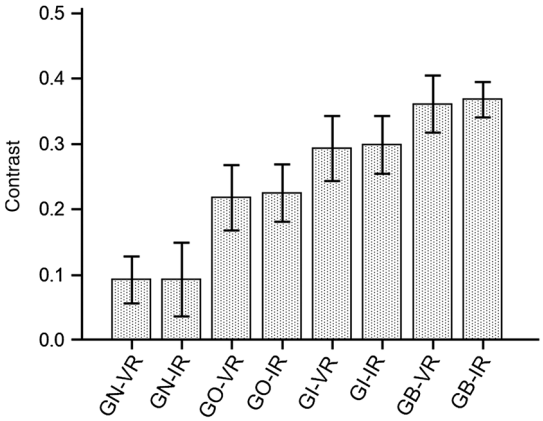

Fig. 4 The contrast of image according to each group.

3 Results

3.1 *GN Group*

The shade of the letter inside the auditory ossicle was not transilluminated in the GN group when observed with VR and IR (GN-VR, GN-IR in Fig. 3). The maximum and minimum grayscales of GN-VR were 246.4 ± 5.7 and 205.1 ± 15.6, respectively. The maximum and minimum grayscales of GN-IR were 239.1 ± 12.9 and 198.7 ± 18.1, respectively. The image contrast of GN-VR and GN-IR were 0.092 ± 0.036 and 0.093 ± 0.057, respectively. There was no statistical difference between GN-VR and GN-IR (Fig. 4).

3.2 *GO Group*

Using VR and IR, it was possible to slightly observe the letter inside the auditory ossicle in the GO group. It was hard to see the long process of incus (GO-VR, GO-IR in Fig. 3). There was no difference between the observation results using VR and the observation results using IR. The maximum and minimum grayscales of GO-VR were 249.5 ± 5.1 and 160.7 ± 15.7, respectively. The maximum and minimum grayscales of GO-IR were 247.9 ± 5.6 and 157.2 ± 13.4, respectively. The image contrast of GO-VR and GO-IR were 0.217 ± 0.049 and 0.224 ± 0.043, respectively. There was no statistical difference between GO-VR and GO-IR. However, there was a statistically significant difference between GN and GO groups (Fig. 4).

3.3 *GI Group*

Using VR and IR, the letter inside the auditory ossicle was distinctively observed in the GI group. Furthermore, the letter inside the long process of incus was distinctively observed when compared with the results obtained for the GO group observation (GI-VR, GI-IR in Fig. 3). There was no difference between the observation results using VR and the observation results using IR. The maximum and minimum grayscales of GI-VR were 248.9 ± 6.8 and 136.5 ± 15.1, respectively. The maximum and minimum grayscales of GI-IR were 246.5 ± 9.7 and 133.6 ± 14.8, respectively. The image contrast of GI-VR and GI-IR were 0.293 ± 0.051 and 0.298 ± 0.044, respectively. There was no statistical difference between GI-VR and GI-IR. However, there was a statistically significant difference between GO and GI groups (Fig. 4).

3.4 *GB Group*

When the GB group was observed with VR, a more distinctive letter image could be obtained in comparison to what was possible with the GO group and the GI group. In the GB group, even the incudostapedial joint could be verified (GB-VR in Fig. 3). When the GB group was observed with IR, it was possible to obtain the most distinctive image. In addition to the incudostapedial joint, the stapedial tendon and the footplate of the stapes, which was located in the innermost portion of middle ear, could be verified (GB-IR in Fig. 3). The maximum and minimum grayscales of GB-VR were 247.7 ± 5.8 and 116.6 ± 11.9, respectively. The maximum and minimum grayscales of GB-IR were 250.5 ± 5.1 and 115.9 ± 8.2, respectively. The image contrasts of GB-VR and GB-IR were 0.361 ± 0.043 and 0.367 ± 0.027, respectively. There was no statistical difference between GB-VR and GB-IR. However, there was a statistically significant difference between GI and GB groups (Fig. 4).

3.5 *Analysis of Image Contrast*

The degree of image contrast increased as following order GN < GO < GI < GB. There was a statistically significant difference between each group (Fig. 4).

4 Discussion

Light is used in medicine for the diagnosis and treatment of diseases. Light transmittance is determined by the degree of light scattering and absorption in a tissue. Scattering defines spectral and angular characteristics of light interacting with living objects, as well as its penetration depth.[6] Light transmittance is increased as the light scattering is reduced.[3] In general, the scattering of a tissue is dependent on refractive index mismatch between cellular tissue components. For fibrous tissue (eye scleral and corneal stroma, skin dermis, muscle, vessel wall, female breast fibrous component, cartilage, tendon, etc.), refractive index mismatching of interstitial medium and long strands of scleroprotein (collagen-, elastin-, or reticulin-forming fibers) are important.[7]

The tympanic membrane is a vital feature of the human ear, and is a thin, circular layer of tissue that marks the point between the middle ear and the external part of the ear. It is ~0.1 − mm thick, and around a third of an inch in diameter. The tympanic membrane is composed of three layers: the outer epithelial layer, the middle fibrous layer, and inner mucosal layer. The main refractive index mismatching of tympanic membrane might arise from fibrous layer. The fibrous layer of tympanic membrane was composed of collagen fibers. Collagen fibers have complex self-assembled structures and are the major scattering centers in tissues.[8] They are widely distributed in different tissues and especially abundant in the dermis of the skin and sclera of the eye. When a high-concentration matching material with a refractive index similar to that of collagen fiber is used, the optical clearing of the tympanic membrane can be improved because the light scattering is reduced. The known refractive index of collagen fiber ranges between 1.45 and 1.504 and glycerol (1.456) has a refractive index in this range making it a biocompatible material, among possible refractive index matching.[9] Hypodermic injection of glycerol can make it easier to observe blood vessels by reducing the light scattering of the skin.[4,10] The results from the tissue optical clearing study can also be applied to other tissues, such as muscle[11] or gastrointestinal tract.[12]

Genina et al.[13] reviewed the optical immersion method based on refractive index matching of scatterers (collagen and elastin fibers, cells and cell compartments) and the ground material (interstitial fluid and/or cytoplasm) of tissue and blood under the action of exogenous optical clearing agents. Such control leads to essential reduction of scattering, and therefore causes much higher transmittance (optical clearing), allowing for successful application of different diagnostic and therapeutic techniques. The optical immersion of glycerol will match the refractive index of tympanic membrane, thus reduce scattering. This is regarded as the major mechanism of glycerol.[13,14] If the refractive index of tympanic membrane could be measured *in vivo* with a refractometer, the refractive index matching would be more accurate. In other words, the structure of the middle ear could be observed more distinctively if the RIM was applied with a refractive index exactly matching that of the tympanic membrane.

Furthermore, other mechanisms of optical clearing of glycerol are dissociation of collagen fibers and are caused by glycerol have been proposed to explain the mechanism of optical clearing based on experimental results. Yeh and Hirshburg[8] studied collagen dissociation by glycerol and reported that glycerol plays the role of reducing light scattering by collagen *in vitro*. However, Wen et al.[15] investigated the optical clearing effect of glycerol and changes in structures of skin during the process of optical clearing were measured. They showed that the reflectance decrease and the thickness of dermis and diameter of collagen fibers decrease. There is no collagen fiber dissociation or fracture with *in vivo* skin. They concluded that the thickness decrease of dermis and regular arrangement of tissue fibers plays an important role in the mechanism for glycerol induced optical clearing of skin *in vivo*. The change in collagen structure and size can lead to a substantial reduction in tissue light scattering. It was concluded that the collagen dissociation is an important mechanism of *in vitro* optical clearing, but the decrease in size is that of *in vivo* optical clearing.[16] Different results could be due to a difference between *in vivo* and *in vitro* skins. Therefore, the collagen dissociation of glycerol might have little relation in this study although we did not verify histopathology.

Another mechanism of glycerol is tissue dehydration. Vargas et al.[4] applied glycerol onto the skin surface and observed the transillumination rate over time. They reported that 20 min after application of the glycerol, the optical clearing was higher than the optical clearing observed in the ears checked 1 and 5 min after the glycerol had been applied. Therefore, 20 min may be the time required for tissue dehydration. This length of time might be required in skin that needs a great deal of dehydration. Yu et al.[17] developed a partial least-squares regression model based on reflectance spectra in the range from 1100 to 1700 nm to quantitatively investigate the dehydration of skin. The authors concluded that dehydration is the main mechanism of skin optical clearing for 1,2-propanediol, 1,4-butanediol during 60-min topical treatment, whereas for glycerol, or D-sorbitol, there should exist other mechanisms that lead to further clearing besides the dehydration. The effect of the glycerol-induced optical clearing was immediate in this study. Therefore, the dehydration mechanism of glycerol might have no relation in this study.

An IR ray is used in various medical fields[18,19] because it results in less scattering and offers high transillumination on the surface of the skin when compared with visible light (wave length 400 to 600 nm). Furthermore, since a CCD camera can detect both visible light and near-IR rays, an IR CCD camera can distinguish information from the mucosa layer and the submucosa layer. The IR CCD camera is used to determine a hemorrhage site or to check the surgical margins of a malignancy with indocyanine green staining dye that absorbs IR rays well.[20–22] Additionally, since the IR CCD camera can distinguish temperature difference, its use makes it possible to distinguish the blood vessels from other tissues, neither of which are easily seen using a general light source during laparascope.[23] An IR ray also increases the image sensitivity by reducing the boundary effect. Our study verified that the image became clearer as the image sensitivity increased when the IR CCD camera was used together with the RIM. However, in the group in which the RIM was not applied, no advantage was found in using IR over VR. Slightly clearer images were obtained in GO and GI groups, but these were not distinctive enough to help diagnosis. However, in the GB group, even the footplate of the stapes, the innermost part of middle ear, could be identified, thus showing that IR can provide images of the deeper

regions of the ear, although there was no statistical difference between GB-VR and GB-IR in the contrast of image.

Clinically, for an RIM to be considered ideal, it should be safe and completely compatible with the human body, it should be easily eliminated and bring about reversible change to the middle ear mucosa or the tympanic membrane. Additionally, its refractive index should be similar to that of the tympanic membrane and a good effect should be found only when the RIM is injected into the outside of the tympanic membrane. Considering all these conditions, glycerol might be the most appropriate RIM because it has a refractive index that is similar to collagen, and it is safe for the human body. Glycerol is also used for the diagnosis of Meniere's disease,[24] since intravenous injection of glycerol brings about temporary hearing improvement by an osmotic change in the inner ear. No cases have been cited in which glycerol was directly used in the middle ear, but glycerol could be safely administered into the inner ear.

In order to apply the results of our study in a clinical setting, several variables and problems must be resolved. Further studies should be conducted to apply glycerol to the tympanic membrane well and investigate the effects of liposoluble cerumen, glycerol concentration, and application duration. Studies focusing on transillumination at different wavelengths should be carried out by increasing the radiation intensity of the 830-nm IR used in this study or by using a near-IR ray with a different wavelength.

5 Conclusion

We observe successfully the middle ear structure using glycerol as the RIM. The optical clearing of tympanic membrane is most effective in GB group, followed by GI and GO groups. The IR camera can be helpful to observe the innermost portion of middle ear in GB group. This method may become a useful alternative method for diagnosis of middle ear disease.

References

1. M. Kraft et al., "Clinical value of optical coherence tomography in laryngology," *Head. Neck.* **30**(12), 1628–1635 (2008).
2. T. Just et al., "Optical coherence tomography of the oval window niche," *J. Laryngol. Otol.* **123**(6), 603–608 (2009).
3. J. Wang et al., "Evaluation of optical clearing with the combined liquid paraffin and glycerol mixture," *Biomed. Opt. Express* **2**(8), 2329–2338 (2011).
4. G. Vargas et al., "Use of an agent to reduce scattering in skin," *Lasers. Surg. Med.* **24**(2), 133–141 (1999).
5. G. Wyszecki and W. S. Stiles, *Color Science. Concepts and Methods, Quantitative Data and Formulae*, 2nd ed., Wiley-Interscience, New York (1982).
6. V. V. Tuchin et al., "Optical clearing of tissues and cells," *J. Biomed. Opt.* **13**(2), 021101 (2008).
7. V. V. Tuchin et al., *Optical Polarization in Biomedical Applications*, Springer-Verlag, New York (2006).
8. Y. T. Yeh and J. Hirshburg, "Molecular interactions of exogenous chemical agents with collagen-implication for tissue optical clearing," *J. Biomed. Opt.* **11**(1), 014003 (2006).
9. X. J. Wang et al., "Group refractive index measurement of dry and hydrated type I collagen films using optical low-coherence reflectometry," *J. Biomed. Opt.* **1**(2), 212–216 (1996).
10. B. Choi et al., "Determination of chemical agent optical clearing potential using in vitro human skin," *Lasers Surg. Med.* **36**(2), 72–75 (2005).
11. S. Plotnikov et al., "Optical clearing for improved contrast in second harmonic generation imaging of skeletal muscle," *Biophys. J.* **90**(1), 328–339 (2006).
12. Y. He and R. K. Wang, "Dynamic optical clearing effect of tissue impregnated with hyperosmotic agents and studied with optical coherence tomography," *J. Biomed. Opt.* **9**(1), 200–206 (2004).
13. E. A. Genina et al., "Tissue optical immersion clearing," *Expert Rev. Med. Devices* **7**(6), 825–842 (2010).
14. V. V. Tuchin et al., "Light propagation in tissues with controlled optical properties," *J. Biomed. Opt.* **2**(4), 401–417 (1997).
15. X. Wen et al., "In vivo skin optical clearing by glycerol solution: mechanism," *J. Biophotonics* **3**(1–2), 44–52 (2010).
16. D. Zhu et al., "Recent progress in tissue optical clearing," *Laser Photonics Rev.* **7**(5), 732–757 (2013).
17. T. Yu et al., "Quantitative analysis of dehydration in porcine skin for assessing mechanism of optical clearing," *J. Biomed. Opt.* **16**(9), 095002 (2011).
18. Y. Zhang et al., "Visible and near-infrared spectroscopy for distinguishing malignant tumor tissue from benign tumor and normal breast tissues in vitro," *J. Biomed. Opt.* **18**(7), 077003 (2013).
19. U. Mahmood et al., "Near-infrared imaging of the sinuses: preliminary evaluation of a new technology for diagnosing maxillary sinusitis," *J. Biomed. Opt.* **15**(3), 036011 (2010).
20. Y. H. El-Sharkawy and A. F. El-Sherif, "High-performance near-infrared imaging for breast cancer detection," *J. Biomed. Opt.* **19**(1), 016018 (2014).
21. T. Kimura et al., "Infrared fluorescence endoscopy for the diagnosis of superficial gastric tumors," *Gastrointest. Endosc.* **66**(1), 37–43 (2007).
22. R. Ishihara et al., "Infrared endoscopic system for detection of bleeding points during endoscopic resection," *Endoscopy* **39**(Suppl 1), E329–E330 (2007).
23. W. W. Roberts et al., "Laparoscopic infrared imaging," *Surg. Endosc.* **11**(12), 1221–1223 (1997).
24. T. Basel and B. Lütkenhöner, "Auditory threshold shifts after glycerol administration to patients with suspected Menière's disease: a retrospective analysis," *Ear Hear.* **34**(3), 370–384 (2013).

Biographies of the authors are not available.